

Article

Investigating the Impacts of Urbanization on PM_{2.5} Pollution in the Yangtze River Delta of China: A Spatial Panel Data Approach

Liang Cheng ^{1,2} , Ting Zhang ¹, Longqian Chen ^{1,*}, Long Li ^{1,3} , Shangjiu Wang ⁴, Sai Hu ⁵, Lina Yuan ¹, Jia Wang ¹ and Mingxin Wen ¹

¹ School of Public Policy and Management, China University of Mining and Technology, Daxue Road 1, Xuzhou 221116, China; liang.cheng@cumt.edu.cn (L.C.); tingzhang@cumt.edu.cn (T.Z.); long.li@cumt.edu.cn or long.li@vub.be (L.L.); lnyuan@cumt.edu.cn (L.Y.); jia.wang@cumt.edu.cn (J.W.); mingxin.wen@cumt.edu.cn (M.W.)

² Henry Fok College of Biology and Agriculture, Shaoguan University, Daxue Road 26, Shaoguan 512005, China

³ Department of Geography, Earth System Science, Vrije Universiteit Brussel, Pleinlaan 2, 1050 Brussels, Belgium

⁴ School of Mathematics and Statistics, Shaoguan University, Daxue Road 26, Shaoguan 512005, China; wangshangjiu@163.com

⁵ School of Humanities and Law, Jiangsu Ocean University, Cangwu Road 59, Lianyungang 222005, China; saihu@jou.edu.cn

* Correspondence: chenlq@cumt.edu.cn; Tel.: +86-516-8359-1327

Received: 12 September 2020; Accepted: 2 October 2020; Published: 4 October 2020



Abstract: Urbanization is a key determinant of fine particulate matter (PM_{2.5}) pollution variability. However, there is a limited understanding of different urbanization factors' roles in PM_{2.5} pollution. Using satellite-derived PM_{2.5} data from 2002 to 2017, we investigated the spatiotemporal evolution and the spatial autocorrelation of PM_{2.5} pollution in the Yangtze River Delta (YRD) region. Afterwards, the impacts of three urbanization factors (population urbanization, land urbanization and economic urbanization) on PM_{2.5} pollution were estimated by a spatial Durbin panel data model (SDM). Obtained results showed that: (i) PM_{2.5} pollution was larger in the north than in the south of YRD; (ii) Lianyungang and Yancheng cities had significant increasing trends in PM_{2.5} pollution from 2002 to 2017; (iii) the regional median center of PM_{2.5} pollution was observed in the Nanjing city, with gradual shifting to the northwest during the 16-year period; (iv) PM_{2.5} pollution showed significant and positive spatial autocorrelation and spillover effect; (v) population urbanization contributed more to the increase in PM_{2.5} pollution than land urbanization, while economic urbanization had no significant impact. The present study highlights the impacts of three urbanization factors on PM_{2.5} pollution which represent valuable and relevant information for air pollution control and urban planning.

Keywords: urbanization; PM_{2.5}; spatial Durbin panel data model; spillover effect; Yangtze River Delta

1. Introduction

Fine particulate matter (PM_{2.5}) mostly originates from anthropogenic activities such as construction, traffic, industrial production, cooking, waste incineration, biomass burning, etc. [1,2]. With small diameter and strong toxicological properties, PM_{2.5} can easily enter into the human body and induce cardiovascular and respiratory diseases [3–5]. Moreover, high levels of PM_{2.5} reduce atmospheric visibility and disturb the earth's radiative balance [6,7]. Recently, numerous urban areas in China have suffered frequent heavy PM_{2.5} pollution [8]. For instance, two large-scale and long-lasting haze

episodes affected central and eastern China between January and December 2013 [9]. These PM_{2.5} pollution episodes have resulted in severe impairments of human health and economic growth in China, thus gaining worldwide attention.

Urbanization, a complex and dynamic process characterized by population migration, urban expansion, landscape change and economic development [10,11], is considered to be closely associated with air quality [12–15]. The aggregation of the population in urban areas (i.e., population urbanization) may result in intensive human activities and huge energy consumption generating massive pollution emissions and deteriorating air quality [16,17]. Meanwhile, during the expansion of built-up areas (i.e., land urbanization), natural lands (e.g., forest land and grassland) are transformed into urban construction lands that may impair the air purification ability of the ecosystem and may contribute to the accumulation of particulate matter [18–20]. However, urban expansion also has a dilution effect on pollutants because high-pollution enterprises are often forced to transfer their activities from the urban core to fringe areas [21]. Economic growth (i.e., economic urbanization) affects the PM_{2.5} concentration in different ways. On one hand, economic development will cause a rise in productive activities while the production with low energy efficiency will often cause massive emissions of air contaminants [22]. On the other hand, the booming economy can provide financial support for environmental governance and technological innovation as well as raising people's environmental protection awareness, which in return lowers the risk of haze [23–25]. Hence, the various forms of urbanization can have different roles in PM_{2.5} pollution and it is thus critical to detect the multiple impacts of different urbanization factors on PM_{2.5} pollution.

Several approaches, including ordinary least squares (OLS) method [26–28], correlation analysis [29,30], input-output analysis [31–33], quantile regression [34–36], geographically weighted regression [37–39] and geographic detector model [40], have been used to detect the impact factors of air pollution. However, the aforementioned methods overlook the spillover effects of air pollutants. In fact, owing to the effect of atmospheric circulation, the PM_{2.5} pollution in a particular city may influence the PM_{2.5} concentrations in nearby cities, which is defined as the spillover effect [41]. Recently, spillover effects were analyzed by using the spatial regression models that add spatial lag or (and) error items in the analyses of the driving forces of air pollution [41–45]. For example, in China, Liu et al. [41] employed the spatial Durbin model (SDM) to examine the factors behind air pollution at the prefecture-level in 2014. Subsequently, Du et al. [45] applied the same model to detect the effects of different urbanization levels on PM_{2.5} pollution at the county-level in 2000 and 2010. However, only cross-sectional data were used in these studies. The panel data provide more information, degrees of freedom, sample variability and less collinearity when compared to cross-sectional data [46]. Thus, the spatial regression models based on the panel data can provide more reliable results than the spatial regression models based on the cross-sectional data [47].

Yangtze River Delta (YRD) is a fast urbanizing region in China that experienced severe haze pollution in recent decades. Concerning the variation of PM_{2.5} concentration in the YRD, Yun et al. [48] used the geographic detector model to detect the impact factors at three time points. In addition, Yang et al. [49] used a traditional spatial panel data model to examine how PM_{2.5} pollution responded to urbanization. However, the aforementioned studies limited the analysis at the cross-sectional data or only considered the impact of urbanization from a single dimension [48,49]. Moreover, both studies overlooked the spillover effect of atmospheric pollutants.

The present study combined the panel data and spatial regression models with the focus on different roles of three urbanization factors (population urbanization, land urbanization and economic urbanization) in PM_{2.5} pollution in the YRD during the period 2002–2017. The primary objectives are to: (i) illustrate the spatiotemporal evolution of PM_{2.5} pollution; (ii) examine the possibilities of spatial autocorrelation for PM_{2.5} pollution; and (iii) investigate the impacts of different urbanization factors on PM_{2.5} pollution with a suitable spatial panel data model.

2. Data and Methods

2.1. Study Area

The YRD (27.20° N–35.33° N, 114.90° E–123.17° E) is located in eastern China (Figure 1a). According to the “Outline of the integrated regional development of the Yangtze River Delta”, there are 41 cities in the area, including 13 cities in Jiangsu Province, 11 cities in Zhejiang Province, 16 cities in Anhui Province, and Shanghai city (Figure 1b; Table S1). The YRD covers approximately 357,282 km² with a population of 223 million in 2017. The area has diverse relief, from plains and deltas in the north and east to low hills and mountains in the south and west. Affected by the monsoon climate, the YRD has abundant precipitation and four distinct seasons. During the 2002–2017 period, the YRD has grown rapidly in urban population, built-up area and gross regional product with annual growth rates of 3.49%, 5.74% and 11.25%, respectively. However, along with the accelerated urbanization, the YRD has been plagued by heavy PM_{2.5} pollution [50]. Consequently, there is a pressing need to explore the impacts of urbanization on PM_{2.5} pollution for guiding the atmospheric pollution governance.

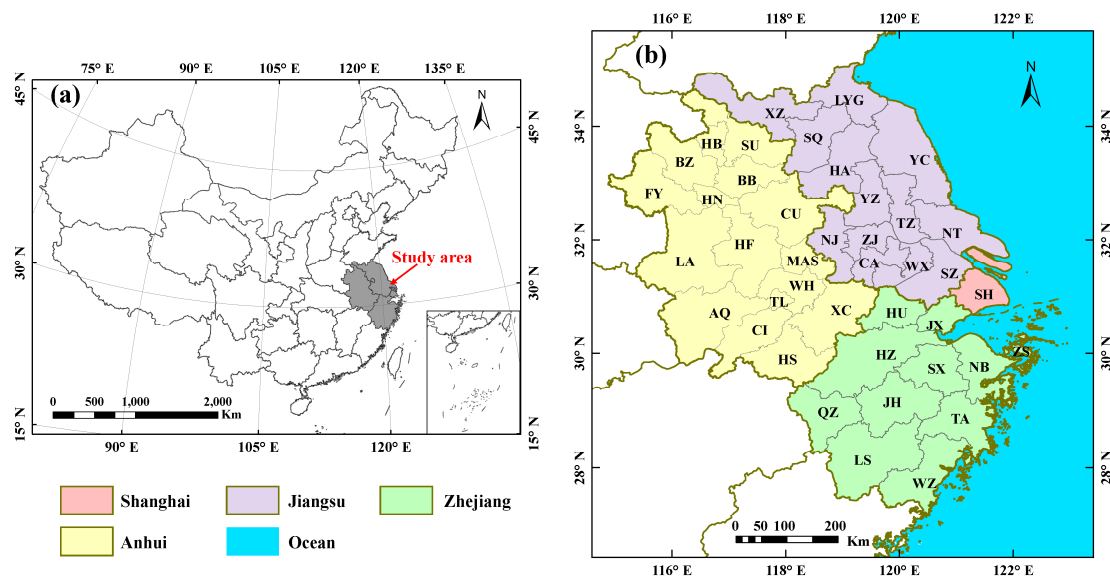


Figure 1. Study area: (a) location of the Yangtze River Delta (YRD) in China; (b) the 41 cities of the YRD (full names of the cities are listed in Table S1). The administrative boundary layer with a scale of 1:250,000 was obtained from the Data Center for Resources and Environmental Sciences, Chinese Academy of Sciences [51].

2.2. Data

Firstly, the overall spatial pattern and dynamics of PM_{2.5} pollution were analyzed at the pixel-level. Then, we examined the spatial dependence of PM_{2.5} pollution by spatial autocorrelation analysis and explored the impacts of urbanization on PM_{2.5} pollution by spatial regression analysis, both of which were conducted at the city-level. Accordingly, the pixel-level and city-level annual PM_{2.5} data were prepared for further analyses (more details in Section 2.2.1). Regarding the impacts of urbanization on PM_{2.5} pollution, we mainly focused on three common forms of urbanization: population urbanization, land urbanization and economic urbanization. These urbanization forms can be expressed by the ratio of urban population, the ratio of urban built-up area and per capita gross regional product, respectively [11]. For the purpose of reducing omitted variable bias, we also considered secondary industry, vegetation coverage, precipitation and wind speed in spatial regression analysis [41,52]. Table 1 lists the specific definitions of all variables, while data sources for the PM_{2.5} concentration and the seven explanatory variables are presented in Sections 2.2.1 and 2.2.2, respectively.

Table 1. Description of the variables.

Variable	Abbreviation	Definition	Unit
PM _{2.5}	PM	Concentration of PM _{2.5}	µg/m ³
Ratio of urban population	PU	Urban population/total population	%
Ratio of urban built-up area	LU	Urban built-up area/city area	%
Per capita gross regional product	EU	Gross regional product/total population	10 ⁴ Yuan
Secondary industry	SI	Secondary industry output/ gross regional product	%
Vegetation coverage	NDVI	Normalized differential vegetation index	n.a.
Precipitation	Prec	Annual precipitation	mm
Wind speed	Wind	Annual average wind speed	m/s

2.2.1. PM_{2.5} Data

The annual PM_{2.5} dataset at a grid resolution of about 1 km was obtained from the Dalhousie University Atmospheric Composition Analysis Group for the period 2002–2017 [53]. The PM_{2.5} data were produced by integrating multiple types of information, including satellite retrievals, simulations, and ground measurements [54–56]. The dataset has relatively high accuracy ($R^2 = 0.81$) [54] and was widely used at different spatial scales [12,16,57]. For the analyses of the spatiotemporal evolution of PM_{2.5} pollution at the pixel-level, the original gridded PM_{2.5} data (a resolution of 1 km) was employed. For the analyses of spatial autocorrelation and spatial regression at the city-level, the mean PM_{2.5} values for each city were calculated based on administrative boundaries.

2.2.2. Urbanization and Other Factors

Data for seven explanatory variables for the period 2002–2017 were gathered from multiple sources. Urbanization and industrial information that includes the ratio of urban population, the ratio of urban built-up area, per capita gross regional product and secondary industry, were collected from the China City Statistical Yearbook (2003–2018) [58]. Notably, the per capita gross regional product data were converted to constant 2002 prices (Chinese Yuan) using GDP deflator [59]. The annual normalized differential vegetation index (NDVI) data with a 1 km spatial resolution, reflecting vegetation growth and coverage, were provided by the Data Center for Resources and Environmental Sciences, Chinese Academy of Sciences [51]. The annual precipitation and average wind speed from meteorological stations in and around the YRD were derived from the China Meteorological Data Service Center [60]. The original meteorological measurements were interpolated to 1 km grid using the inverse distance weighting method in order to generate continuous surfaces of precipitation and wind speed [40]. In addition, NDVI, precipitation and wind speed were averaged within administrative boundaries for each city.

2.2.3. Variables Selection

For the spatial regression analysis in Section 2.3.4, all variables, including PM, PU, LU, EU, SI, NDVI, Prec and Wind (See Table 1 for their full names and descriptions) were appropriated natural logarithmic forms to reduce the potential heteroscedasticity (Table S2). In addition, variance inflation factors (VIF) were calculated for the seven explanatory variables. Obtained VIF values are less than 10 (Table S3), thus suggesting that the explanatory variables exhibit no multi-collinearity [61,62].

2.3. Methods

2.3.1. Trend Analysis

The nonparametric Mann–Kendall test is powerful in identifying the significant trend in time series data [63–66] and the nonparametric Sen’s slope estimator [67,68] provides a robust estimate of the slope. Compared with the parametric approaches, nonparametric approaches are distribution free, less affected by outliers, and hence more applicable for time series analysis [69,70]. In this study, the Mann–Kendall and Sen’s slope tests were used to identify trends in PM_{2.5} time series from 2002 to

2017. Firstly, for each pixel, we performed the Mann-Kendall test to detect whether the PM_{2.5} time series has a significant trend. If the p-value is less than 0.05, the corresponding trend is considered significant [71]. Then, the slope values of the PM_{2.5} data were calculated by performing Sen's slope test in order to indicate the direction and the magnitude of the temporal changes in PM_{2.5} concentration. The two tests were performed by using the trend package in R software (version 3.2.2, R Foundation for Statistical Computing, Vienna, Austria).

2.3.2. Standard Deviation Ellipse Analysis

We employed the standard deviation ellipse (SDE) method to depict the spatial pattern changes of PM_{2.5} pollution during 2002–2017. Three basic parameters of the SDE, including median center, long-short axis ratio and azimuth, were used to measure the dispersion and directional tendencies of elements in our study [72]. The median center is the point that has a minimum sum of distances to all the elements, thus identifying the location where the elements are most concentrated [73]. Accordingly, the change in the median center can reflect the overall moving trace of elements. The long and short half axes illustrate the primary and secondary distribution direction of the elements. The long-short axis ratio (i.e., the ratio of the lengths of the long axis to the short axis), an indicator describing the shape of an ellipse, can determine whether the elements are densely distributed in a certain direction or evenly distributed in the ellipse. The smaller the value, the less probability the elements are concentrated in a certain direction [74]. The azimuth, which ranges from 0 to 180 degrees, refers to the angle deviating clockwise from the north direction to the long axis direction, revealing the leading direction of elements [75]. The SDE analysis was performed by using the median center and directional distribution tools in ArcGIS software (version 10.2, ESRI Inc., Redlands, CA, USA).

2.3.3. Spatial Autocorrelation Analysis

Spatial autocorrelation means that the nearby observations of a variable tend to be positively or negatively correlated [76]. To examine the necessity of constructing spatial regression models, we assessed the spatial autocorrelation of PM_{2.5} pollution in the YRD using global Moran's I [77]. The Moran's I ranges from −1 to 1: a) when $0 < \text{Moran's I} < 1$, it denotes a positive spatial autocorrelation and a clustering pattern of PM_{2.5} pollution, b) when $-1 < \text{Moran's I} < 0$, it denotes a negative spatial autocorrelation and a dispersion pattern of PM_{2.5} pollution and c) when $\text{Moran's I} = 0$, it denotes a random spatial distribution. The p-value reflects the significance level and additional details about this method can be found in the literature [78,79]. In this study, the global Moran's I of PM_{2.5} pollution for each year between 2002 and 2017 was estimated based on the inverse distance spatial weight matrix [80,81] by employing the spatial autocorrelation tool in ArcGIS software (version 10.2, ESRI Inc., Redlands, CA, USA).

2.3.4. Spatial Regression Analysis

To cope with the potential spatial dependence in PM_{2.5} pollution among the cities, we considered three types of spatial regression models when analyzing the impacts of urbanization on PM_{2.5} pollution [82]. The first model is the spatial lag model (SLM), which includes a spatially lagged dependent variable and hypothesizes that the PM_{2.5} pollution in the city i is influenced by the PM_{2.5} pollution in the neighboring cities [83]. In our case, the SLM model can be established as follows:

$$\ln PM_{it} = \beta_1 \ln PU_{it} + \beta_2 \ln LU_{it} + \beta_3 \ln EU_{it} + \beta_4 \ln SI_{it} + \beta_5 \ln NDVI_{it} + \beta_6 \ln Prec_{it} + \beta_7 \ln Wind_{it} + \rho W \ln PM_{it} + \mu_i + \xi_t + \varepsilon_{it} \quad (1)$$

where $\beta_1, \beta_2, \dots, \beta_7$ represent the seven regression coefficients of the explanatory variables; ρ denotes the spatial autoregressive coefficient measuring the intensity of spatial dependence in PM_{2.5} pollution among cities; W stands for the spatial weight matrix, which is the inverse distance spatial weight

matrix in this case; μ_i and ξ_t correspond to spatial effect and time effect, respectively. ε_{it} is a normally distributed random error terms.

The second model is the spatial error model (SEM), which contains a lagged error term and hypothesizes that the errors in neighboring cities are likely to interact. It can be constructed as follows:

$$\begin{aligned} \ln PM_{it} = & \beta_1 \ln PU_{it} + \beta_2 \ln LU_{it} + \beta_3 \ln EU_{it} + \beta_4 \ln SI_{it} + \beta_5 \ln NDVI_{it} \\ & + \beta_6 \ln Prec_{it} + \beta_7 \ln Wind_{it} + \mu_i + \xi_t + \phi_{it} \\ \phi_{it} = & \lambda W \phi_{it} + \varepsilon_{it} \end{aligned} \quad (2)$$

where ϕ_{it} represents the spatial autocorrelation error term; λ is the spatial autocorrelation coefficient of the error term.

The third model is the spatial Durbin model (SDM), which incorporates both the spatially lagged dependent variable and explanatory variables, considering not only the spatial dependence of the dependent variable but also that of the explanatory variables [84,85]. It can be defined as follows:

$$\begin{aligned} \ln PM_{it} = & \beta_1 \ln PU_{it} + \beta_2 \ln LU_{it} + \beta_3 \ln EU_{it} + \beta_4 \ln SI_{it} + \beta_5 \ln NDVI_{it} + \beta_6 \ln Prec_{it} \\ & + \beta_7 \ln Wind_{it} + \theta_1 W \ln PU_{it} + \theta_2 W \ln LU_{it} + \theta_3 W \ln EU_{it} + \theta_4 W \ln SI_{it} \\ & + \theta_5 W \ln NDVI_{it} + \theta_6 W \ln Prec_{it} + \theta_7 W \ln Wind_{it} + \rho W \ln PM_{it} + \mu_i + \xi_t + \varepsilon_{it} \end{aligned} \quad (3)$$

where $\theta_1, \theta_2, \dots, \theta_7$ refer to the spatial lag coefficients of the explanatory variables.

Several model tests help to select an appropriate spatial regression model. Following the standard approach proposed by Elhorst [86], the spatial regression analysis starts with a non-spatial model estimated by OLS. Afterwards, the Likelihood ratio (LR) joint significance test can be performed in order to determine whether the model should control for spatial fixed or time fixed effects [86]. In this study, the random effect was not considered because the analysis focuses on the population rather than the sample [87]. Then, the Lagrange multiplier (LM) tests and Robust LM tests can be used to investigate whether there exist spatial interaction effects in dependent variables or errors. If the result justifies the existence of the spatial interaction effect, the SDM model is recommended to be established [85]. In this case, to access whether the SDM can be degraded into SLM or SEM, the Wald and LR tests should be carried out. By contrast, if there are no spatial interaction effects, the spatial regression model should not be selected.

The above spatial models can be estimated by the maximum likelihood (ML) method. Notably, since the SLM and SDM involve spatial lags of the dependent variable, the coefficients of explanatory variables (i.e., $\beta_1, \beta_2, \dots, \beta_7$) in the two models could not represent the marginal effect [83]. Therefore, direct and indirect effects coefficients should be further estimated. In this study, the direct effect refers to the impact on $PM_{2.5}$ pollution of the city i resulted from a change in an explanatory variable of the city i . The indirect (spillover) effect illustrates the cumulative impacts on $PM_{2.5}$ pollution caused by changes in an explanatory variable of other cities. The sum of the two effects is the total effect. More details about the estimation of the direct and indirect effects can be found in LeSage and Pace [85]. The spatial regression analysis was performed in the MATLAB software (version R2016a, MathWorks Inc., Natick, MA, USA).

3. Results

3.1. Spatial Pattern of $PM_{2.5}$ Pollution

The distinct spatial variation in the 16-year mean (from 2002 to 2017) $PM_{2.5}$ concentrations in the YRD is presented in Figure 2. It can be noticed that the $PM_{2.5}$ concentrations in the larger part of YRD (83.57%) exceeded the World Health Organization (WHO) Interim target-1 ($35 \mu\text{g}/\text{m}^3$), thus suggesting severe haze pollution in this region. The maximum, average and minimum $PM_{2.5}$ concentrations were $74.87 \mu\text{g}/\text{m}^3$, $49.15 \mu\text{g}/\text{m}^3$ and $19.24 \mu\text{g}/\text{m}^3$, respectively. Overall, it can be noticed that $PM_{2.5}$ pollution is heavier in the north than in the south. The extremely high $PM_{2.5}$ concentrations ($>65 \mu\text{g}/\text{m}^3$)

were concentrated in Xuzhou (XZ), Suzhou (SuZ), Huaibei (HB), Bozhou (BZ) and Fuyang (FY) cities, accounting for 4.91% of the YRD area. In contrast, relatively low $PM_{2.5}$ concentrations ($<25 \mu\text{g}/\text{m}^3$) were noticed mainly in Lishui (LS) and Wenzhou (WZ) cities, accounting for only 2.36% of the area.

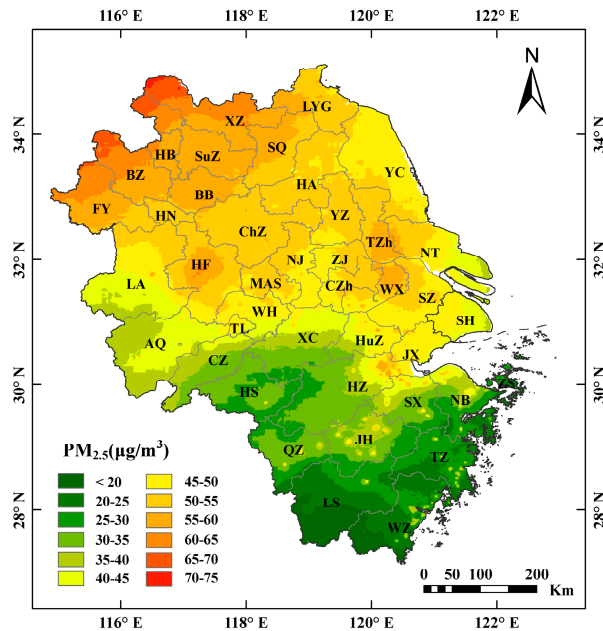


Figure 2. The 16-year mean $PM_{2.5}$ values in the YRD from 2002 to 2017.

3.2. Trends of $PM_{2.5}$ Concentrations

The significance levels (i.e., p -values) and slopes of the trends in $PM_{2.5}$ concentrations were calculated by methods mentioned in Section 2.3.1. Figure 3a shows the p -values of the upward (slope > 0) and downward (slope < 0) trends, while Figure 3b shows the slopes of the trends. The results showed that approximately 16.12% and 0.98% of the study area had significant ($p < 0.05$) upward and downward trends, respectively (Figure 3a). The north and central YRD were characterized by upward trends with larger parts of Lianyungang (LYG) and Yancheng (YC) cities having the greatest concentration growth (slope > 1.2) at a high significance level ($p < 0.01$) (Figure 3b). Xuzhou (XZ), Huai'an (HA), Yangzhou (YZ) and Taizhou (TZ) cities also witnessed the significant increase in $PM_{2.5}$ concentration with slope values exceeding 0.9 in larger parts of these cities. By contrast, downward trends were noticed in the south YRD with most slopes being not significant ($p \geq 0.05$). Only a few parts of the Lishui (LS) and Quzhou (QZ) cities illustrated significant ($p < 0.05$) decrease (slope < 0) in $PM_{2.5}$ concentration.

Figure 4 demonstrates the four standard deviational ellipses of $PM_{2.5}$ pollution in 2002, 2007, 2012 and 2017. In addition, Table 2 displays the basic parameters of the ellipses. The median center of the pollution was found in northwestern Nanjing city (Figure 4), moving from 118.63° E and 31.87° N in 2002 to 118.50° E and 32.01° N in 2017 (Table 2). The moving directions and the rates of the median center in the three five-year intervals could be computed according to its coordinates (Table 2). From 2002 to 2007, the median center moved to the northwest at a speed of 2.8 km/year. Afterwards, it shifted slowly to the southeast at a speed of 1.8 km/year during the period 2007–2012. From 2012 to 2017, the median center shifted quickly towards the northwest at a speed of 3.2 km/year. The shapes of a series of ellipses indicated that $PM_{2.5}$ pollution was clustered mainly in the “southeast-northwest” direction (Figure 4). The long-short axis ratio reduced gradually from 1.604 to 1.545 during the period 2002–2017 (Table 2), reflecting that the directionality of the $PM_{2.5}$ pollution was weakened and that the dispersion of pollution decreased in the long axis direction (i.e., “southeast-northwest”) and expanded in the short axis direction (i.e., “northeast-southwest”). Furthermore, the azimuth changed only slightly

from 143.58° to 143.97° (Table 2), which indicated that the leading direction of PM_{2.5} concentrations had no distinct change.

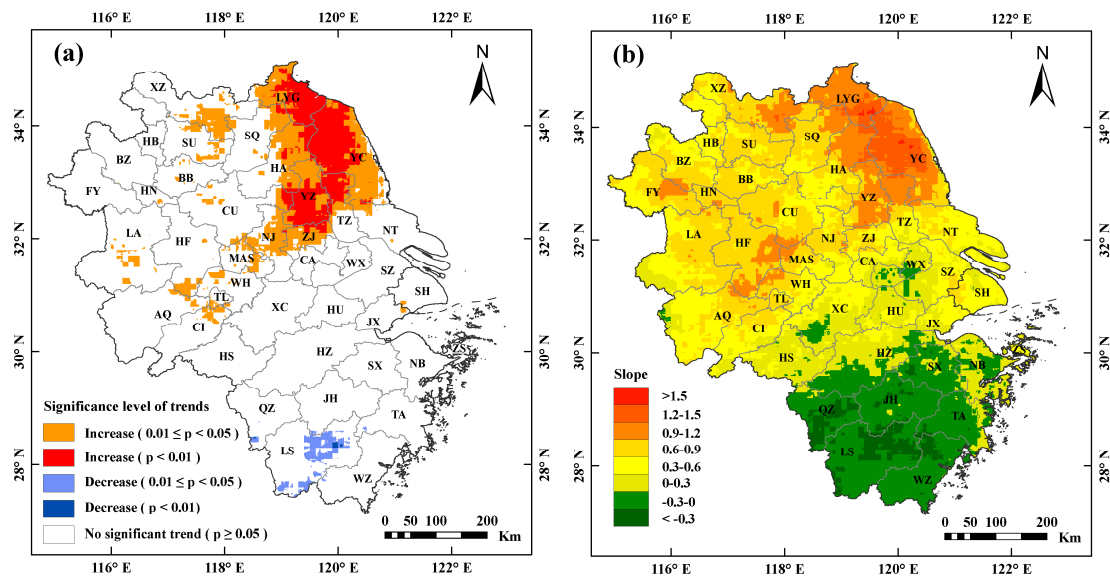


Figure 3. Trends in PM_{2.5} concentrations during 2002–2017 period: (a) significance level of trends (increase means slope >0 and decrease means slope <0); and (b) slope values.

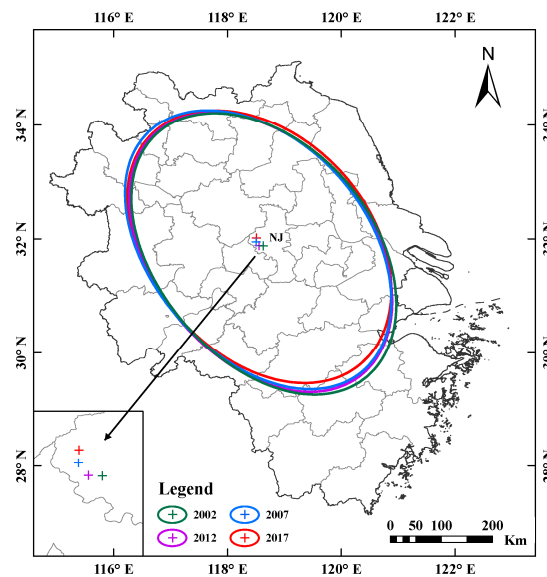


Figure 4. Standard deviational ellipses of PM_{2.5} pollution in 2002, 2007, 2012 and 2017. The cross marks denote the median centers of the ellipses.

Table 2. Median centers, long-short axis ratios and azimuths of the standard deviational ellipses in 2002, 2007, 2012 and 2017.

Year	Longitude of the Median Center (°)	Latitude of the Median Center (°)	Long-short Axis Ratio	Azimuth (°)
2002	118.63	31.87	1.604	143.93
2007	118.50	31.94	1.602	143.58
2012	118.55	31.87	1.591	144.31
2017	118.50	32.01	1.545	143.97

3.3. Spatial Autocorrelation Analysis

Table 3 presents the global Moran’s I values of PM_{2.5} pollution during the period 2002–2017. Obtained values were positive and significant ($p < 0.01$), suggesting positive spatial autocorrelation in PM_{2.5} pollution. Additionally, the Moran’s I exhibited an upward trend in general, with values 0.242 in 2002, 0.316 in 2010, and 0.292 in 2017, thus showing a strengthening spatial clustering trend in PM_{2.5} pollution. Accordingly, the spatial regression models should be considered in the subsequent analysis.

Table 3. Global Moran’s I values of PM_{2.5} pollution over the YRD during the period 2002–2017.

Year	Moran’s I	Year	Moran’s I
2002	0.242 ***	2010	0.316 ***
2003	0.245 ***	2011	0.279 ***
2004	0.225 ***	2012	0.252 ***
2005	0.246 ***	2013	0.276 ***
2006	0.280 ***	2014	0.279 ***
2007	0.266 ***	2015	0.281 ***
2008	0.242 ***	2016	0.300 ***
2009	0.264 ***	2017	0.292 ***

Note: *** $p < 0.01$.

3.4. Spatial Panel Regression Analysis

3.4.1. Results of Model Tests

Table 4 reports the results of the spatial diagnostic tests for non-spatial regression models. The results of the LR joint significance tests provided evidence about the existence of the spatial fixed effects (1370.892, $p < 0.01$) and time fixed effects (722.186, $p < 0.01$). This indicated that the panel data model including both the spatial and time effects was a suitable choice. Regarding the type of spatial regression model, as demonstrated in the first four rows (Table 4), the LM tests and Robust LM tests were statistically significant ($p < 0.05$) for all the model specifications. This result implies that the spatial interaction effects in both dependent variables and error terms could not be neglected. Thus, by following the general-to-specific approach, we established the SDM model with spatial and time fixed effects and subsequently implemented the Wald and LR tests. As highlighted in Table 5, all statistics of Wald and LR tests were significant at 1% level, which verified the superiority of SDM over SLM and SEM. Accordingly, the SDM model under the spatial and time fixed effects was chosen to describe the data, and the subsequent analysis was based on it.

Table 4. Results of spatial diagnostic tests for non-spatial panel models.

Test	Pooled OLS	Spatial Fixed Effects	Time Fixed Effects	Spatial and Time Fixed Effects
LM (lag)	885.512 ***	1642.571 ***	319.747 ***	303.322 ***
LM (error)	1241.314 ***	1688.130 ***	141.319 ***	250.414 ***
Robust LM (lag)	4.637 **	102.611 ***	241.033 ***	74.353 ***
Robust LM (error)	360.439 ***	331.666 ***	62.606 ***	21.445 ***
LR joint significance test for spatial fixed effect				1370.892 ***
LR joint significance test for time fixed effect				722.186 ***

Note: ** $p < 0.05$, *** $p < 0.01$.

Table 5. Results of Wald and LR tests for the spatial Durbin model under the spatial and time fixed effects.

Test	Wald Test (SDM Versus SLM)	LR Test (SDM Versus SLM)	Wald Test (SDM Versus SEM)	LR Test (SDM Versus SEM)
Statistics	89.839 ***	84.280 ***	112.479 ***	103.978 ***

Note: *** $p < 0.01$.

3.4.2. Estimation Results

The SDM model was fitted with the maximum likelihood (ML) estimator by considering the spatial and time fixed effects (Table 6). The spatial autoregressive coefficient ρ is highly significant ($p < 0.01$) with a value of 0.867, thus indicating a strong link between the PM_{2.5} pollution in neighboring cities.

Table 6. Results of the SDM model under the spatial and time fixed effects.

Variable	Value	Variable	Value
lnPU	0.105 **	W×lnLU	0.546 ***
lnLU	0.055 *	W×lnEU	−0.322
lnEU	−0.028	W×lnSI	0.408 ***
lnSI	0.043 *	W×lnNDVI	−1.928 ***
lnNDVI	−0.209 *	W×lnPrec	−0.007
lnPrec	−0.024	W×lnWind	0.490
lnWind	−0.326	ρ	0.867 ***
W×lnPU	1.405 ***	R ²	0.970

Note: * $p < 0.1$, ** $p < 0.05$, *** $p < 0.01$; W×lnPU, W×lnLU, W×lnEU, W×lnSI, W×lnNDVI, W×lnPrec, W×lnWind denote the spatial lags of lnPU, lnLU, lnEU, lnSI, lnNDVI, lnPrec and lnWind, respectively.

Due to the feedback effect, the spatial regression coefficients cannot truly illustrate the marginal effects of urbanization, secondary industry, NDVI, precipitation and wind speed. Hence, we further computed the direct, indirect and total effects of each variable on PM_{2.5} pollution (Table 7). Four variables (i.e., lnPU, lnLU, lnSI and lnNDVI) showed significant total effects with the coefficients of 4.084, 2.182, 1.379 and −5.988, respectively. For the direct effect, lnPU had the largest significant positive coefficient (0.310), followed by lnLU (0.149) and lnSI (0.116), suggesting that every 1% increase in lnPU, lnLU and lnSI will directly increase lnPM by 0.310%, 0.149%, and 0.116% in the local city, respectively. In contrast, lnNDVI, lnPrec and lnWind had negative direct effects with the respective coefficients of −0.541, −0.031 and −0.283, thus implying that NDVI, precipitation and wind speed exerted direct negative impacts on PM_{2.5} pollution. By considering the indirect effect, lnPU, lnLU and lnSI showed significant and positive indirect effects. Specifically, every 1% growth in these three variables in nearby cities can increase lnPM by 3.774%, 2.033% and 1.263% in the local city, respectively. Moreover, lnNDVI had a considerable high negative and significant indirect effect (−5.447). For the lnEU, which represented the economic urbanization, neither the direct effect nor the indirect effect was significant.

Table 7. Direct, indirect and total effects of the seven explanatory variables.

Variable	Direct Effect	Indirect Effect	Total Effect
lnPU	0.310 ***	3.774 ***	4.084 ***
lnLU	0.149 ***	2.033 ***	2.182 ***
lnEU	−0.079	−1.245	−1.324
lnSI	0.116 ***	1.263 ***	1.379 ***
lnNDVI	−0.541 ***	−5.447 ***	−5.988 ***
lnPrec	−0.031 **	−0.223	−0.254
lnWind	−0.283 **	1.512	1.229

Note: *** $p < 0.01$.

4. Discussion

4.1. The Impacts of Urbanization on $PM_{2.5}$ Pollution

The present study highlighted the different impacts of the three forms of urbanization on $PM_{2.5}$ pollution for the YRD during the study period (Table 7). Complying with the previous studies [41,45,88], population urbanization played a dominant role in increasing $PM_{2.5}$ pollution and land urbanization was also a large contributor to $PM_{2.5}$ pollution. Regarding economic urbanization, some studies argued that it can lead to an increase in $PM_{2.5}$ concentration [12,47]. However, it showed a negative and insignificant impact on $PM_{2.5}$ levels in the YRD. Based on our results, the underlying mechanisms that different forms of urbanization impact $PM_{2.5}$ pollution are illustrated in Figure 5.

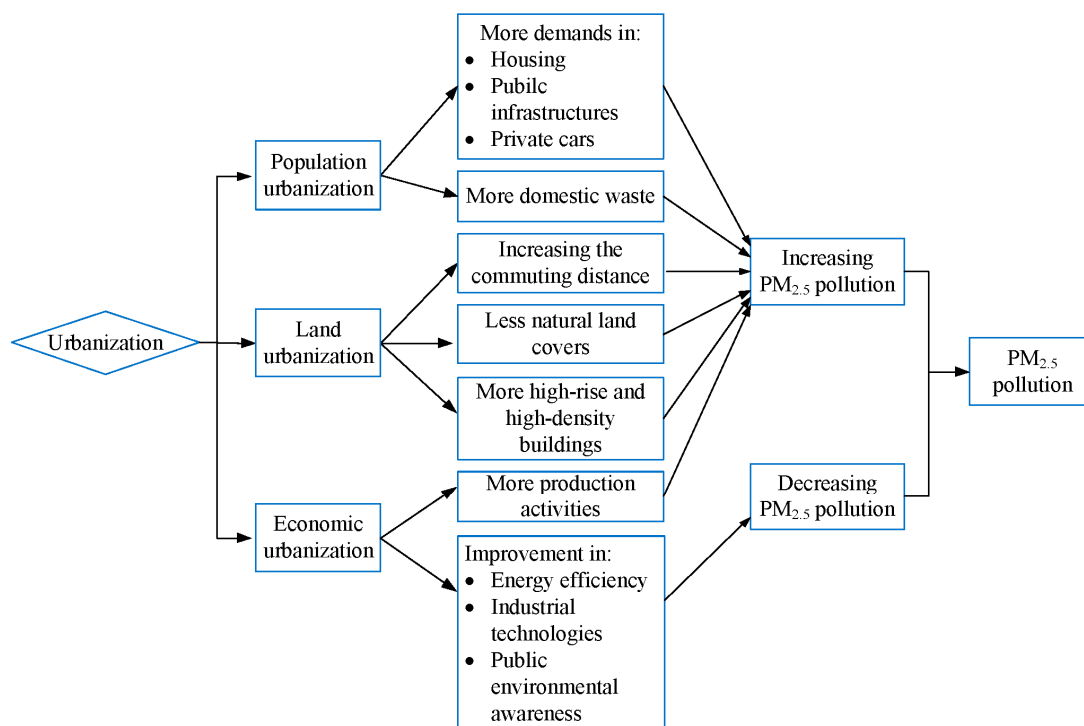


Figure 5. The impact mechanisms of urbanization on $PM_{2.5}$ pollution.

Population urbanization describes the migration of the population from rural areas to urban areas, mainly impacting $PM_{2.5}$ pollution in two ways. On one hand, the urban population agglomeration is usually accompanied by high demands for new housing, public infrastructures and private cars, which will inevitably raise energy consumption [12]. The growing energy consumption contributes to increased exhaust emissions, thereby enhancing air pollution. On the other hand, as the population increases and the people's living standards improve, large amounts of domestic waste are produced in the urban area. The released aerosol particles due to the improper garbage disposal may further increase $PM_{2.5}$ concentration [10].

Land urbanization refers to the process of urban sprawl. The impact of land urbanization on $PM_{2.5}$ pollution may be explained in three aspects. Firstly, the larger the built-up area, the longer the commuting distance for residents, which will increase the traffic flows [89]. As a consequence, emissions from vehicles will contribute substantially to $PM_{2.5}$ pollution. Secondly, the majority of the natural land covers (e.g., forest land and grassland) are replaced by artificial surfaces during the land urbanization process. Compared with artificial surfaces, forest and grass can purify the air through obstructing and absorbing the particulate matter. Accordingly, land cover changes may weaken the self-purification ability of urban ecosystems [18]. Lastly, the high-rise and high-density buildings can hinder the dilution and dispersion of air pollutants [90].

Economic urbanization can be regarded as the process of economic growth. It influences PM_{2.5} pollution from opposite directions. For one thing, rapid economic growth can induce more production activities that leads to increased pollution emissions [45]. For another thing, economic urbanization is usually accompanied by the increased energy efficiency, improved industrial technologies and raised public environmental awareness, which can alleviate air pollution. Consequently, the final statistically insignificant direct and indirect effect coefficients of economic urbanization in the YRD may be attributed to the dual effects of economic urbanization. Liu et al. [41] also found that per capita GDP had no significant influence on air quality.

4.2. The Impacts of other Factors on PM_{2.5} Concentrations

In addition to urbanization factors, we have introduced the secondary industry, NDVI, precipitation and wind speed into our model to reduce the omitted variable bias. The results showed that the secondary industry enhanced PM_{2.5} levels (Table 7), which is in accordance with a previous study [47]. That is because the secondary industry, especially heavy industry and real estate, consume large amounts of energy and generates high concentrations of atmospheric pollutants. Vegetation coverage (Table 7), represented by NDVI, is able to partially absorb and block particulate matter [6], which contributed to the decline in PM_{2.5} concentrations. Additionally, precipitation and wind speed played important roles in mitigating the local PM_{2.5} pollution (Table 7) as precipitation can remove the particles by wet deposition while wind facilitates the dispersion of particles [91].

4.3. Policy Implications

The findings from this empirical study contributed to the development of policy implications with the aim to alleviate PM_{2.5} pollution.

Firstly, the spillover effect of PM_{2.5} pollution implies that inter-regional cooperation is necessary for preventing, mitigating and controlling air pollution. Accordingly, an information sharing system should be established at the regional level with the aim to provide the information related to air quality monitoring, pollution emissions and emergency response to air pollution accidents [92]. Meanwhile, unified environmental laws and regulations should be formulated and implemented to restrict the transfer of pollution among cities [12].

Secondly, governments should emphasize on the popularization of non-fossil fuel energy and citizen's environmental awareness. As demonstrated by the results, the growth in urban population and built-up area contributed substantially to the energy consumption and air pollutant emissions, thereby increasing PM_{2.5} concentration. Hence, it is crucial to reduce coal consumption and encourage the usage of clean energy [88]. In addition, enhancing green consumption, promoting the use of public transportation and advocating garbage classification can increase the public's awareness of air protection [11].

Finally, attention should be devoted to industrial structure and urban planning. It is urgent to close the highly polluting industry, transform the traditional industries with advanced technologies and to encourage the development of green industry [12]. In addition, the impacts of vegetation coverage, precipitation and wind speed on PM_{2.5} concentration should not be overlooked. To reduce the risk of air pollution exposure, urban planning measures should be adopted that include designing urban ventilation corridors, allocating large scale green space in the downwind direction of pollution source and arranging suitable tree species in the street [93].

4.4. Limitation

This present study has a few limitations. Firstly, the used socioeconomic data employed were derived based on the administrative boundaries, which may, to a certain extent, impact the estimation results. To more accurately characterize urbanization, grid data (e.g., satellite-derived nighttime light data and population data) should be considered in the follow-up studies. Secondly, the analysis was conducted at the annual time scale with the emphasis on detecting the impacts of urbanization on

PM_{2.5} pollution. Accordingly, the influencing mechanisms of precipitation and wind speed on air pollution could not be revealed completely and it would be beneficial to perform the spatial regression analysis on shorter time scales (e.g., day, month and season).

5. Conclusions

The present study analyzed the spatiotemporal evolution of PM_{2.5} pollution at the pixel-level in the YRD from 2002 to 2017. Then, the spatial autocorrelation of PM_{2.5} pollution among the 41 cities in the study domain was examined. Finally, we investigated the impacts of different urbanization factors (population urbanization, land urbanization and economic urbanization) on PM_{2.5} pollution at the city-level. The key findings from this study are as follows:

- Distinct variation in the spatial pattern of the PM_{2.5} concentrations was identified in the YRD. Approximately 83.57% of the YRD had mean PM_{2.5} concentrations higher than 35 µg/m³ (WHO Interim Target 1). The pollution was more severe in the north than in the south part of the YRD.
- The significant and largest increasing trends in PM_{2.5} pollution was noticed in Lianyungang and Yancheng cities. However, the regional median center of the PM_{2.5} pollution was located in the Nanjing city and was gradually shifting to the northwest during the research period.
- The positive spatial autocorrelation and spillover effect of PM_{2.5} pollution were verified by the global Moran's I values and the SDM model, respectively, thus suggesting that the prevention and control of air pollution should rely on inter-regional cooperation.
- Population urbanization, land urbanization, secondary industry and NDVI exerted significant impacts on PM_{2.5} pollution. Population urbanization had the largest positive total effect, followed by land urbanization and secondary industry, while NDVI showed a negative total effect. No significant effect was detected for economic urbanization.

In general, we have noticed that the impact mechanisms of different forms of urbanization on PM_{2.5} pollution varied. The investigation of these impact mechanisms can help policymakers and urban planners in developing measures to abate air pollution.

Supplementary Materials: The following are available online at <http://www.mdpi.com/2073-4433/11/10/1058/s1>, Table S1: The abbreviations and belonged provinces of cities in the YRD; Table S2: The descriptive statistics of variables; Table S3: Results of VIF test.

Author Contributions: Conceptualization, L.C. (Liang Cheng), T.Z. and L.L.; methodology, L.C. (Liang Cheng) and S.W.; software, S.W. and S.H.; validation, T.Z. and L.Y.; formal analysis, L.C. (Liang Cheng); data curation, J.W. and M.W.; writing—original draft preparation, L.C. (Liang Cheng); writing—review and editing, L.L. and L.C. (Longqian Chen); visualization, L.C. (Liang Cheng); supervision, project administration and funding acquisition, L.C. (Longqian Chen). All authors have read and agreed to the published version of the manuscript.

Funding: This research was funded by the Fundamental Research Funds for the Central Universities (Grant No.: 2018ZDPY07).

Conflicts of Interest: The authors declare no conflict of interest.

References

1. Hallquist, M.; Wenger, J.C.; Baltensperger, U.; Rudich, Y.; Simpson, D.; Claeys, M.; Dommen, J.; Donahue, N.M.; George, C.; Goldstein, A.H.; et al. The formation, properties and impact of secondary organic aerosol: Current and emerging issues. *Atmos. Chem. Phys.* **2009**, *9*, 5155–5236. [[CrossRef](#)]
2. Zhang, R.; Jing, J.; Tao, J.; Hsu, S.C.; Wang, G.; Cao, J.; Lee, C.S.L.; Zhu, L.; Chen, Z.; Zhao, Y.; et al. Chemical characterization and source apportionment of PM_{2.5} in Beijing: Seasonal perspective. *Atmos. Chem. Phys.* **2013**, *13*, 7053–7074. [[CrossRef](#)]
3. Dominici, F.; Peng, R.D.; Bell, M.L.; Pham, L.; McDermott, A.; Zeger, S.L.; Samet, J.M. Fine particulate air pollution and hospital admission for cardiovascular and respiratory diseases. *JAMA* **2006**, *295*, 1127. [[CrossRef](#)] [[PubMed](#)]

4. Fann, N.; Lamson, A.D.; Anenberg, S.C.; Wesson, K.; Risley, D.; Hubbell, B.J. Estimating the national public health burden associated with exposure to ambient PM_{2.5} and ozone. *Risk Anal.* **2012**, *32*, 81–95. [CrossRef]
5. Hoek, G.; Krishnan, R.M.; Beelen, R.; Peters, A.; Ostro, B.; Brunekreef, B.; Kaufman, J.D. Long-term air pollution exposure and cardio-respiratory mortality: A review. *Environ. Health* **2013**, *12*, 43. [CrossRef]
6. Aklesso, M.; Kumar, K.R.; Bu, L.; Boiyo, R. Analysis of spatial-temporal heterogeneity in remotely sensed aerosol properties observed during 2005–2015 over three countries along the Gulf of Guinea Coast in Southern West Africa. *Atmos. Environ.* **2018**, *182*, 313–324. [CrossRef]
7. Pui, D.Y.H.; Chen, S.-C.; Zuo, Z. PM_{2.5} in China: Measurements, sources, visibility and health effects, and mitigation. *Particuology* **2014**, *13*, 1–26. [CrossRef]
8. Zhang, Y.; Shuai, C.; Bian, J.; Chen, X.; Wu, Y.; Shen, L. Socioeconomic factors of PM_{2.5} concentrations in 152 Chinese cities: Decomposition analysis using LMDI. *J. Clean. Prod.* **2019**, *218*, 96–107. [CrossRef]
9. Ministry of Environmental Protection of the People’s Republic of China. Report on the state of the environment in China, 2013. Available online: <http://english.mee.gov.cn/Resources/Reports/soe/Report/201706/P020170614504782926467.pdf> (accessed on 1 April 2020).
10. Liang, L.; Wang, Z.; Li, J. The effect of urbanization on environmental pollution in rapidly developing urban agglomerations. *J. Clean. Prod.* **2019**, *237*, 117649. [CrossRef]
11. Zhou, C.; Wang, S.; Wang, J. Examining the influences of urbanization on carbon dioxide emissions in the Yangtze River Delta, China: Kuznets curve relationship. *Sci. Total Environ.* **2019**, *675*, 472–482. [CrossRef]
12. Zhu, W.; Wang, M.; Zhang, B. The effects of urbanization on PM_{2.5} concentrations in China’s Yangtze River Economic Belt: New evidence from spatial econometric analysis. *J. Clean. Prod.* **2019**, *239*, 118065. [CrossRef]
13. Civerolo, K.; Hogrefe, C.; Lynn, B.; Rosenthal, J.; Ku, J.Y.; Solecki, W.; Cox, J.; Small, C.; Rosenzweig, C.; Goldberg, R.; et al. Estimating the effects of increased urbanization on surface meteorology and ozone concentrations in the New York City metropolitan region. *Atmos. Environ.* **2007**, *41*, 1803–1818. [CrossRef]
14. De Ridder, K.; Lefebvre, F.; Adriaensen, S.; Arnold, U.; Beckroege, W.; Bronner, C.; Damsgaard, O.; Dostal, I.; Dufek, J.; Hirsch, J.; et al. Simulating the impact of urban sprawl on air quality and population exposure in the German Ruhr area. Part II: Development and evaluation of an urban growth scenario. *Atmos. Environ.* **2008**, *42*, 7070–7077. [CrossRef]
15. Martins, H. Urban compaction or dispersion? An air quality modelling study. *Atmos. Environ.* **2012**, *54*, 60–72. [CrossRef]
16. Han, L.; Zhou, W.; Li, W.; Qian, Y. Urbanization strategy and environmental changes: An insight with relationship between population change and fine particulate pollution. *Sci. Total Environ.* **2018**, *642*, 789–799. [CrossRef] [PubMed]
17. Baklanov, A.; Molina, L.T.; Gauss, M. Megacities, air quality and climate. *Atmos. Environ.* **2016**, *126*, 235–249. [CrossRef]
18. Lu, D.; Xu, J.; Yue, W.; Mao, W.; Yang, D.; Wang, J. Response of PM_{2.5} pollution to land use in China. *J. Clean. Prod.* **2020**, *244*, 118741. [CrossRef]
19. Manes, F.; Marando, F.; Capotorti, G.; Blasi, C.; Salvatori, E.; Fusaro, L.; Ciancarella, L.; Mircea, M.; Marchetti, M.; Chirici, G.; et al. Regulating Ecosystem Services of forests in ten Italian Metropolitan Cities: Air quality improvement by PM₁₀ and O₃ removal. *Ecol. Indic.* **2016**, *67*, 425–440. [CrossRef]
20. Janhäll, S. Review on urban vegetation and particle air pollution - Deposition and dispersion. *Atmos. Environ.* **2015**, *105*, 130–137. [CrossRef]
21. Feng, Y.; Wang, X. Effects of urban sprawl on haze pollution in China based on dynamic spatial Durbin model during 2003–2016. *J. Clean. Prod.* **2020**, *242*, 118368. [CrossRef]
22. Du, Y.; Sun, T.; Peng, J.; Fang, K.; Liu, Y.; Yang, Y.; Wang, Y. Direct and spillover effects of urbanization on PM_{2.5} concentrations in China’s top three urban agglomerations. *J. Clean. Prod.* **2018**, *190*, 72–83. [CrossRef]
23. Sohag, K.; Begum, R.A.; Abdullah, S.M.S.; Jaafar, M. Dynamics of energy use, technological innovation, economic growth and trade openness in Malaysia. *Energy* **2015**, *90*, 1497–1507. [CrossRef]
24. Fan, X.; Xu, Y. Convergence on the haze pollution: City-level evidence from China. *Atmos. Pollut. Res.* **2020**, *11*, 141–152. [CrossRef]
25. Dong, F.; Zhang, S.; Long, R.; Zhang, X.; Sun, Z. Determinants of haze pollution: An analysis from the perspective of spatiotemporal heterogeneity. *J. Clean. Prod.* **2019**, *222*, 768–783. [CrossRef]
26. Wu, J.; Zhang, P.; Yi, H.; Qin, Z. What causes haze pollution? An empirical study of PM_{2.5} concentrations in Chinese cities. *Sustainability* **2016**, *8*, 132. [CrossRef]

27. Lee, C. Impacts of urban form on air quality: Emissions on the road and concentrations in the US metropolitan areas. *J. Environ. Manag.* **2019**, *246*, 192–202. [[CrossRef](#)]
28. Jiménez-Parra, B.; Alonso-Martínez, D.; Godos-Díez, J.L. The influence of corporate social responsibility on air pollution: Analysis of environmental regulation and eco-innovation effects. *Corp. Soc. Responsib. Environ. Manag.* **2018**, *25*, 1363–1375. [[CrossRef](#)]
29. Han, L.; Zhou, W.; Li, W.; Li, L. Impact of urbanization level on urban air quality: A case of fine particles (PM_{2.5}) in Chinese cities. *Environ. Pollut.* **2014**, *194*, 163–170. [[CrossRef](#)]
30. Botlaguduru, V.S.V.; Kommalapati, R.R. Meteorological detrending of long-term (2003–2017) ozone and precursor concentrations at three sites in the Houston Ship Channel Region. *J. Air Waste Manag. Assoc.* **2020**, *70*, 93–107. [[CrossRef](#)]
31. Alcántara, V.; Padilla, E.; Piaggio, M. Nitrogen oxide emissions and productive structure in Spain: An input–output perspective. *J. Clean. Prod.* **2017**, *141*, 420–428. [[CrossRef](#)]
32. Giannakis, E.; Kushta, J.; Giannadaki, D.; Georgiou, G.K.; Bruggeman, A.; Lelieveld, J. Exploring the economy-wide effects of agriculture on air quality and health: Evidence from Europe. *Sci. Total Environ.* **2019**, *663*, 889–900. [[CrossRef](#)] [[PubMed](#)]
33. Román, R.; Cansino, J.M.; Rueda-Cantuche, J.M. A multi-regional input-output analysis of ozone precursor emissions embodied in Spanish international trade. *J. Clean. Prod.* **2016**, *137*, 1382–1392. [[CrossRef](#)]
34. Del Sarto, S.; Marino, M.F.; Ranalli, M.G.; Salvati, N. Using finite mixtures of M-quantile regression models to handle unobserved heterogeneity in assessing the effect of meteorology and traffic on air quality. *Stoch. Environ. Res. Risk Assess.* **2019**, *33*, 1345–1359. [[CrossRef](#)]
35. Otero, N.; Sillmann, J.; Schnell, J.L.; Rust, H.W.; Butler, T. Synoptic and meteorological drivers of extreme ozone concentrations over Europe. *Environ. Res. Lett.* **2016**, *11*, 024005. [[CrossRef](#)]
36. Schuch, D.; de Freitas, E.D.; Espinosa, S.I.; Martins, L.D.; Carvalho, V.S.B.; Ramin, B.F.; Silva, J.S.; Martins, J.A.; de Fatima Andrade, M. A two decades study on ozone variability and trend over the main urban areas of the São Paulo state, Brazil. *Environ. Sci. Pollut. Res.* **2019**, *26*, 31699–31716. [[CrossRef](#)]
37. Hajiloo, F.; Hamzeh, S.; Gheysari, M. Impact assessment of meteorological and environmental parameters on PM_{2.5} concentrations using remote sensing data and GWR analysis (case study of Tehran). *Environ. Sci. Pollut. Res.* **2019**, *26*, 24331–24345. [[CrossRef](#)]
38. Alahmadi, S.; Al-Ahmadi, K.; Almeshari, M. Spatial variation in the association between NO₂ concentrations and shipping emissions in the Red Sea. *Sci. Total Environ.* **2019**, *676*, 131–143. [[CrossRef](#)]
39. Shi, Y.; Ren, C.; Lau, K.K.-L.; Ng, E. Investigating the influence of urban land use and landscape pattern on PM_{2.5} spatial variation using mobile monitoring and WUDAPT. *Landsc. Urban Plan.* **2019**, *189*, 15–26. [[CrossRef](#)]
40. Cheng, L.; Li, L.; Chen, L.; Hu, S.; Yuan, L.; Liu, Y.; Cui, Y.; Zhang, T. Spatiotemporal variability and influencing factors of aerosol optical depth over the Pan Yangtze River Delta during the 2014–2017 period. *Int. J. Environ. Res. Public Health* **2019**, *16*, 3522. [[CrossRef](#)]
41. Liu, H.; Fang, C.; Zhang, X.; Wang, Z.; Bao, C.; Li, F. The effect of natural and anthropogenic factors on haze pollution in Chinese cities: A spatial econometrics approach. *J. Clean. Prod.* **2017**, *165*, 323–333. [[CrossRef](#)]
42. Balado-Naves, R.; Baños-Pino, J.F.; Mayor, M. Do countries influence neighbouring pollution? A spatial analysis of the EKC for CO₂ emissions. *Energy Policy* **2018**, *123*, 266–279. [[CrossRef](#)]
43. Maddison, D. Modelling sulphur emissions in Europe: A spatial econometric approach. *Oxf. Econ. Pap.* **2007**, *59*, 726–743. [[CrossRef](#)]
44. Marbuah, G.; Amuakwa-Mensah, F. Spatial analysis of emissions in Sweden. *Energy Econ.* **2017**, *68*, 383–394. [[CrossRef](#)]
45. Du, Y.; Wan, Q.; Liu, H.; Liu, H.; Kapsar, K.; Peng, J. How does urbanization influence PM_{2.5} concentrations? Perspective of spillover effect of multi-dimensional urbanization impact. *J. Clean. Prod.* **2019**, *220*, 974–983. [[CrossRef](#)]
46. Elhorst, J.P. *Spatial Econometrics: From Cross-Sectional Data to Spatial Panels*, 1st ed.; Springer: Berlin/Heidelberg, Germany, 2014; pp. 1–3. ISBN 978-3-642-40339-2.
47. Ding, Y.; Zhang, M.; Chen, S.; Wang, W.; Nie, R. The environmental Kuznets curve for PM_{2.5} pollution in Beijing-Tianjin-Hebei region of China: A spatial panel data approach. *J. Clean. Prod.* **2019**, *220*, 984–994. [[CrossRef](#)]

48. Yun, G.; He, Y.; Jiang, Y.; Dou, P.; Dai, S. PM_{2.5} spatiotemporal evolution and drivers in the Yangtze river delta between 2005 and 2015. *Atmosphere (Basel)* **2019**, *10*, 55. [[CrossRef](#)]
49. Yang, D.; Chen, Y.; Miao, C.; Liu, D. Spatiotemporal variation of PM_{2.5} concentrations and its relationship to urbanization in the Yangtze river delta region, China. *Atmos. Pollut. Res.* **2019**, *11*, 491–498. [[CrossRef](#)]
50. Lu, D.; Mao, W.; Yang, D.; Zhao, J.; Xu, J. Effects of land use and landscape pattern on PM_{2.5} in Yangtze River Delta, China. *Atmos. Pollut. Res.* **2018**, *9*, 705–713. [[CrossRef](#)]
51. RESDC (Data Center for Resources and Environmental Sciences, Chinese Academy of Sciences). Available online: <http://www.resdc.cn> (accessed on 22 October 2019).
52. Zhang, X.; Chen, L.; Yuan, R. Effect of natural and anthropic factors on the spatiotemporal pattern of haze pollution control of China. *J. Clean. Prod.* **2020**, *251*, 119531. [[CrossRef](#)]
53. Atmospheric Composition Analysis Group. Available online: http://fizz.phys.dal.ca/~{}atmos/martin/?page_id=140 (accessed on 18 November 2019).
54. Van Donkelaar, A.; Martin, R.V.; Brauer, M.; Hsu, N.C.; Kahn, R.A.; Levy, R.C.; Lyapustin, A.; Sayer, A.M.; Winker, D.M. Global estimates of fine particulate matter using a combined geophysical-statistical method with information from satellites, models, and monitors. *Environ. Sci. Technol.* **2016**, *50*, 3762–3772. [[CrossRef](#)]
55. Van Donkelaar, A.; Martin, R.V.; Li, C.; Burnett, R.T. Regional estimates of chemical composition of fine particulate matter using a combined geoscience-statistical method with information from satellites, models, and monitors. *Environ. Sci. Technol.* **2019**, *53*, 2595–2611. [[CrossRef](#)] [[PubMed](#)]
56. Van Donkelaar, A.; Martin, R.V.; Brauer, M.; Boys, B.L. Use of satellite observations for long-term exposure assessment of global concentrations of fine particulate matter. *Environ. Health Perspect.* **2015**, *123*, 135–143. [[CrossRef](#)] [[PubMed](#)]
57. Li, J.; Han, X.; Jin, M.; Zhang, X.; Wang, S. Globally analysing spatiotemporal trends of anthropogenic PM_{2.5} concentration and population's PM_{2.5} exposure from 1998 to 2016. *Environ. Int.* **2019**, *128*, 46–62. [[CrossRef](#)] [[PubMed](#)]
58. National Bureau of Statistics of China. *China City Statistical Yearbook (2003–2018)*. Available online: <https://data.cnki.net/yearbook/Single/N2020050229> (accessed on 1 March 2020). (In Chinese).
59. Huang, J.; Liu, C.; Chen, S.; Huang, X.; Hao, Y. The convergence characteristics of China's carbon intensity: Evidence from a dynamic spatial panel approach. *Sci. Total Environ.* **2019**, *668*, 685–695. [[CrossRef](#)]
60. China Meteorological Data Service Center. Available online: <http://data.cma.cn/en> (accessed on 20 November 2019).
61. Li, L.; Zhou, X.; Chen, L.; Chen, L.; Zhang, Y.; Liu, Y. Estimating urban vegetation biomass from Sentinel-2A image data. *Forests* **2020**, *11*, 125. [[CrossRef](#)]
62. Kang, Y.; Zhao, T.; Yang, Y. Environmental Kuznets curve for CO₂ emissions in China: A spatial panel data approach. *Ecol. Indic.* **2016**, *63*, 231–239. [[CrossRef](#)]
63. Kendall, M.G. *Rank Correlation Methods*, 4th ed.; Charles Griffin: London, UK, 1975; ISBN 978 0852641996.
64. Bari, M.A.; Kindzierski, W.B. Eight-year (2007–2014) trends in ambient fine particulate matter (PM_{2.5}) and its chemical components in the Capital Region of Alberta, Canada. *Environ. Int.* **2016**, *91*, 122–132. [[CrossRef](#)]
65. Chatterjee, S.; Khan, A.; Akbari, H.; Wang, Y. Monotonic trends in spatio-temporal distribution and concentration of monsoon precipitation (1901–2002), West Bengal, India. *Atmos. Res.* **2016**, *182*, 54–75. [[CrossRef](#)]
66. Mann, H.B. Nonparametric tests against trend. *Econometrica* **1945**, *13*, 245–259. [[CrossRef](#)]
67. Zhao, N.; Jiao, Y.; Ma, T.; Zhao, M.; Fan, Z.; Yin, X.; Liu, Y.; Yue, T. Estimating the effect of urbanization on extreme climate events in the Beijing-Tianjin-Hebei region, China. *Sci. Total Environ.* **2019**, *688*, 1005–1015. [[CrossRef](#)]
68. Sen, P.K. Estimates of the regression coefficient based on Kendall's tau. *J. Am. Stat. Assoc.* **1968**, *63*, 1379–1389. [[CrossRef](#)]
69. Ribeiro, L.; Kretschmer, N.; Nascimento, J.; Buxo, A.; Rötting, T.; Soto, G.; Señoret, M.; Oyarzún, J.; Maturana, H.; Oyarzún, R. Evaluating piezometric trends using the Mann-Kendall test on the alluvial aquifers of the Elqui River basin, Chile. *Hydrol. Sci. J.* **2015**, *60*, 1840–1852. [[CrossRef](#)]
70. Nyelele, C.; Kroll, C.N. The equity of urban forest ecosystem services and benefits in the Bronx, NY. *Urban For. Urban Green.* **2020**, *53*, 126723. [[CrossRef](#)]
71. Lorelei de Jesus, A.; Thompson, H.; Knibbs, L.D.; Kowalski, M.; Cyrus, J.; Niemi, J.V.; Kousa, A.; Timonen, H.; Luoma, K.; Petäjä, T.; et al. Long-term trends in PM_{2.5} mass and particle number concentrations in urban air: The impacts of mitigation measures and extreme events due to changing climates. *Environ. Pollut.* **2020**, *263*, 114500. [[CrossRef](#)]

72. Peng, J.; Chen, S.; Lü, H.; Liu, Y.; Wu, J. Spatiotemporal patterns of remotely sensed PM_{2.5} concentration in China from 1999 to 2011. *Remote Sens. Environ.* **2016**, *174*, 109–121. [[CrossRef](#)]
73. Shi, Y.; Matsunaga, T.; Yamaguchi, Y.; Zhao, A.; Li, Z.; Gu, X. Long-term trends and spatial patterns of PM_{2.5}-induced premature mortality in South and Southeast Asia from 1999 to 2014. *Sci. Total Environ.* **2018**, *631–632*, 1504–1514. [[CrossRef](#)]
74. Li, H.; Li, L.; Chen, L.; Zhou, X.; Cui, Y.; Liu, Y.; Liu, W. Mapping and characterizing spatiotemporal dynamics of impervious surfaces using Landsat images: A case study of Xuzhou, East China from 1995 to 2018. *Sustainability* **2019**, *11*, 1224. [[CrossRef](#)]
75. Rahman, M.; Yang, R.; Di, L. Clustering Indian Ocean tropical cyclone tracks by the standard deviational ellipse. *Climate* **2018**, *6*, 39. [[CrossRef](#)]
76. Cui, Y.; Li, L.; Chen, L.; Zhang, Y.; Cheng, L.; Zhou, X.; Yang, X. Land-use carbon emissions estimation for the Yangtze River Delta Urban Agglomeration using 1994–2016 Landsat image data. *Remote Sens.* **2018**, *10*, 1334. [[CrossRef](#)]
77. Getis, A. A history of the concept of spatial autocorrelation: A geographer’s perspective. *Geogr. Anal.* **2008**, *40*, 297–309. [[CrossRef](#)]
78. Li, H.; Calder, C.A.; Cressie, N. Beyond Moran’s I: Testing for spatial dependence based on the spatial autoregressive model. *Geogr. Anal.* **2007**, *39*, 357–375. [[CrossRef](#)]
79. Moran, P.A.P. Notes on continuous stochastic phenomena. *Biometrika* **1950**, *37*, 17–23. [[CrossRef](#)] [[PubMed](#)]
80. Glass, A.J.; Kenjegalieva, K.; Sickles, R.C. A spatial autoregressive stochastic frontier model for panel data with asymmetric efficiency spillovers. *J. Econom.* **2016**, *190*, 289–300. [[CrossRef](#)]
81. Li, M.; Li, C.; Zhang, M. Exploring the spatial spillover effects of industrialization and urbanization factors on pollutants emissions in China’s Huang-Huai-Hai region. *J. Clean. Prod.* **2018**, *195*, 154–162. [[CrossRef](#)]
82. Elhorst, J.P. Matlab software for spatial panels. *Int. Reg. Sci. Rev.* **2014**, *37*, 389–405. [[CrossRef](#)]
83. Bottasso, A.; Conti, M.; Ferrari, C.; Tei, A. Ports and regional development: A spatial analysis on a panel of European regions. *Transp. Res. Part A Policy Pract.* **2014**, *65*, 44–55. [[CrossRef](#)]
84. Elhorst, J.P. Applied spatial econometrics: Raising the bar. *Spat. Econ. Anal.* **2010**, *5*, 9–28. [[CrossRef](#)]
85. LeSage, J.; Pace, R.K. *Introduction to Spatial Econometrics*; CRC Press Taylor & Francis Group: Boca Raton, FL, USA, 2009; pp. 45–75. ISBN 9781420064254.
86. Elhorst, J.P. Dynamic spatial panels: models, methods, and inferences. *J. Geogr. Syst.* **2012**, *14*, 5–28. [[CrossRef](#)]
87. Wooldridge, J.M. *Econometric Analysis of Cross Section and Panel Data*, 2nd ed.; The MIT Press: London, UK, 2010; pp. 281–334. ISBN 9780262232586.
88. Wang, X.; Tian, G.; Yang, D.; Zhang, W.; Lu, D.; Liu, Z. Responses of PM_{2.5} pollution to urbanization in China. *Energy Policy* **2018**, *123*, 602–610. [[CrossRef](#)]
89. Stone, B. Urban sprawl and air quality in large US cities. *J. Environ. Manag.* **2008**, *86*, 688–698. [[CrossRef](#)]
90. Weng, Q.; Yang, S. Urban air pollution patterns, land use, and thermal landscape: An examination of the linkage using GIS. *Environ. Monit. Assess.* **2006**, *117*, 463–489. [[CrossRef](#)] [[PubMed](#)]
91. Li, X.; Song, H.; Zhai, S.; Lu, S.; Kong, Y.; Xia, H.; Zhao, H. Particulate matter pollution in Chinese cities: Areal-temporal variations and their relationships with meteorological conditions (2015–2017). *Environ. Pollut.* **2019**, *246*, 11–18. [[CrossRef](#)] [[PubMed](#)]
92. Chen, C.; Sun, Y.; Lan, Q.; Jiang, F. Impacts of industrial agglomeration on pollution and ecological efficiency—A spatial econometric analysis based on a big panel dataset of China’s 259 cities. *J. Clean. Prod.* **2020**, *258*, 120721. [[CrossRef](#)]
93. Guo, L.; Luo, J.; Yuan, M.; Huang, Y.; Shen, H.; Li, T. The influence of urban planning factors on PM_{2.5} pollution exposure and implications: A case study in China based on remote sensing, LBS, and GIS data. *Sci. Total Environ.* **2019**, *659*, 1585–1596. [[CrossRef](#)] [[PubMed](#)]

